ELSEVIER

1 July 2001

Optics Communications 194 (2001) 151–165

OPTICS COMMUNICATIONS

www.elsevier.com/locate/optcom

Dispersive optical bistability in cold atomic vapours

G.R.M. Robb [a,*], B.W.J. McNeil [a], R. Bonifacio [b], N. Piovella [b]

[a] *Department of Physics and Applied Physics, John Anderson Building, University of Strathclyde, Glasgow G4 0NG, Scotland, UK*
[b] *Dipartimento di Fisica, Universitá Degli Studi di Milano, INFN and INFM, Via Celoria 16, I-20133 Milano, Italy*

Received 15 January 2001; accepted 10 April 2001

Abstract

We present an analysis of dispersive optical bistability in a system of cold atoms enclosed in a bidirectional ring cavity. This analysis is carried out using a system of equations which extend the so-called Maxwell–Bloch model to self-consistently include atomic centre-of-mass motion. When the atomic sample is sufficiently cold and dense, the atomic centre-of-mass motion causes the low pump transmission state to become unstable when the pump is blue-shifted with respect to the atomic resonance. This recoil-induced instability results in the exponential growth of the radiation field counterpropagating to the pump and an atomic density grating. The density grating strongly influences the dispersive properties of the atomic sample and causes the pump transmission to jump from the low transmission state to the high transmission state. It is expected that these effects should be observable in a cold ($T < 30\mu$ K), dense ($n \sim 10^{11}$ cm^{-3}) sample of Rb, enclosed in a high quality ring cavity ($R \approx 99\%$).

Keywords: Recoil; Vapor; Bistable; Instability

1. Introduction

An optical system which exhibits two steady transmission states for the same input intensity is said to be optically bistable. In this paper we investigate optical bistability (OB) of a dispersive system of free two-level atoms enclosed in a bidirectional ring cavity. In contrast to previous analyses of dispersive OB [1–3] we include the atomic centre-of-mass motion, which is allowed to evolve in a self-consistent way under the action of the counterpropagating radiation fields within the cavity. Previous work on dispersive OB has only approximated the effects of atomic motion through an inhomogeneous broadening of the atomic transition. While such an approximate description of the atomic centre-of-mass dynamics is sufficient to describe quantum electronic phenomena such as OB in warm atomic vapours, it is inadequate to describe these phenomena in cold atomic media, as collective phenomena arising from the atomic centre-of-mass dynamics can dramatically affect the behaviour of the atom + field system.

Dense atomic vapours with sub-Doppler temperatures are now routinely produced in many laboratories worldwide. Investigations of quantum electronic phenomena in cold atomic media such as this would therefore appear to be timely.

* Corresponding author. Fax: +44-141-552-2891.
E-mail address: g.r.m.robb@strath.ac.uk (G.R.M. Robb).

0030-4018/01/$ - see front matter
PII: S0030-4018(01)01249-4

In previous papers [4,5] we described how the inclusion of atomic centre-of-mass motion affected OB in an absorptive sample of cold atoms. It is well known that experimental observation of absorptive OB is generally more difficult than dispersive OB [6] due to the requirement that the atomic transition must be saturated and the laser frequency must be very stable. It would be expected that dispersive OB would also be the simpler phenomenon to investigate in a cold atomic vapour, as operating far from atomic resonance will allow the neglect of scattering, which would otherwise heat the atoms and could inhibit growth of the collective effects we wish to observe [5].

The structure of the paper is as follows: the model we use to describe dispersive OB in cold atomic vapours is described in some detail in Section 2. It is essentially the same as that of the collective atomic recoil laser (CARL) [7–10] in that it self-consistently describes the internal and external degrees of freedom of a collection of two-level atoms interacting with optical fields. We assume that only two degenerate, counterpropagating cavity modes undergo significant interaction with the atoms. The atoms are contained within a cavity driven unidirectionally by an input pump field which is detuned from both the atomic resonance and the cavity resonance. In Section 3 we show how our model reduces to the original mean-field model of OB [1,2] in a homogeneously broadened atomic medium when atomic centre-of-mass motion is neglected and highlight some significant features of dispersive OB in this limit. In Section 4 we include the effects of atomic centre-of-mass motion, and show using linear analysis and nonlinear numerical analysis that they can dramatically change the bistable behaviour of the pump transmission through the system via a recoil-induced instability which causes the spontaneous growth of an atomic density modulation with a spatial period of half the radiation wavelength. We show how the effects of Doppler broadening can quench the recoil-induced instability and suggest a possible experiment to demonstrate these effects using cold, dense Rb vapour. Finally, we present our conclusions in Section 5.

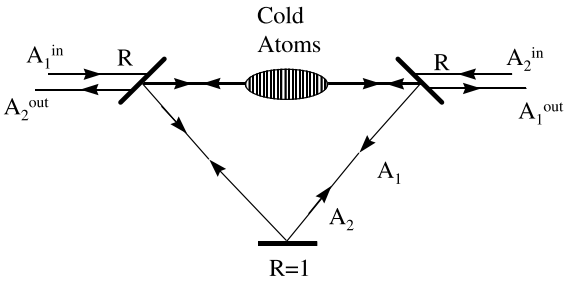

Fig. 1. Schematic diagram of a bidirectional ring cavity.

2. Model

In this section we derive the evolution equations which describe the interaction between an ensemble of two-level atoms and two counterpropagating modes of a bidirectional ring cavity, as shown schematically in Fig. 1. The model used is semi-classical, with the internal atomic degrees of freedom (dipole moment, population difference) described quantum mechanically and the electromagnetic fields and the external atomic degrees of freedom (position, momentum) described classically.

2.1. Electromagnetic field dynamics

Let us assume that the cavity consists of an arrangement of perfectly reflecting mirrors ($R = 1$) and that only one mode is excited in each direction of propagation. In contrast to previous studies using this CARL model [4,5,11–13], we allow both input frequencies to be detuned from those of the cavity modes. The field in the cavity will then be of the form

$$\mathbf{E} = \left(\mathscr{E}_1(t)\mathrm{e}^{\mathrm{i}k_c(z-ct)} + \mathscr{E}_2(t)\mathrm{e}^{-\mathrm{i}k_c(z+ct)} + \text{c.c.}\right)\hat{\mathbf{e}}, \qquad (1)$$

where $\hat{\mathbf{e}}$ is a unit transverse vector and $k_c = 2\pi m/\mathscr{L}$ is the mode wave number, where m is an integer and $\mathscr{L}$ is the cavity length. Maxwell's wave equation is

$$\left(\nabla^2 - \frac{1}{c^2}\frac{\partial^2}{\partial t^2}\right)\mathbf{E} = \frac{1}{\epsilon_0 \mathbf{c}^2}\frac{\partial^2 \mathbf{P}}{\partial \mathbf{t}^2}, \qquad (2)$$

where $\mathbf{P}$ is given by

$$\mathbf{P} = \sum_j \mathbf{d}_j \delta(\mathbf{r} - \mathbf{r}_j),$$

$\mathbf{d}_j$ is the dipole moment of the jth atom, represented by

$$\mathbf{d}_j = \mu\left(S_1(t)\mathrm{e}^{\mathrm{i}k_c(z_j(t)-ct)} + S_2\mathrm{e}^{-\mathrm{i}k_c(z_j(t)+ct)} + \text{c.c.}\right)\hat{\mathbf{e}} \quad (3)$$

and μ is the dipole matrix element.

Assuming the slowly-varying envelope approximation (SVEA) i.e.

$$\left(\frac{\partial^2}{\partial z^2} - \frac{1}{c^2}\frac{\partial^2}{\partial t^2}\right)\left(\mathscr{E}_1\mathrm{e}^{\mathrm{i}k_c(z-ct)}\right) \approx \frac{2\mathrm{i}k_c}{c}\frac{\mathrm{d}\mathscr{E}_1}{\mathrm{d}t}\mathrm{e}^{\mathrm{i}k_c(z-ct)},$$

$$\left(\frac{\partial^2}{\partial z^2} - \frac{1}{c^2}\frac{\partial^2}{\partial t^2}\right)\left(\mathscr{E}_2\mathrm{e}^{-\mathrm{i}k_c(z+ct)}\right) \approx \frac{2\mathrm{i}k_c}{c}\frac{\mathrm{d}\mathscr{E}_2}{\mathrm{d}t}\mathrm{e}^{-\mathrm{i}k_c(z+ct)}$$

and that

$$\frac{\partial^2\mathbf{P}}{\partial t^2} \approx -k_c^2c^2\mathbf{P},$$

then the wave equation (2) becomes

$$\frac{\mathrm{d}\mathscr{E}_1}{\mathrm{d}t}\mathrm{e}^{\mathrm{i}k_cz} + \frac{\mathrm{d}\mathscr{E}_2}{\mathrm{d}t}\mathrm{e}^{-\mathrm{i}k_cz} \approx \frac{\mathrm{i}k_c\mu}{2\epsilon_0}\sum_j\left(S_1(t)\mathrm{e}^{\mathrm{i}k_cz_j} + S_2(t)\mathrm{e}^{-\mathrm{i}k_cz_j}\right)\delta(\mathbf{r}-\mathbf{r}_j). \quad (4)$$

Multiplying Eq. (4) by $\mathrm{e}^{-\mathrm{i}k_cz}$ and integrating over the cross-sectional area of the sample, A, and the cavity length, $\mathscr{L}$, gives

$$\frac{\mathrm{d}\mathscr{E}_1}{\mathrm{d}t} = \frac{\mathrm{i}k_c\mu n}{2\epsilon_0}\left\langle S_1 + S_2\mathrm{e}^{-\mathrm{i}\theta}\right\rangle, \quad (5)$$

where $\langle\cdots\rangle = (1/N)\sum_j^N(\cdots)_j$, $n = N/A\mathscr{L} = n_sL_s/\mathscr{L}$ is the density of atoms in the cavity, L_s is that atomic sample length, $n_s = N/AL_s$ is the atomic sample density and $\theta = 2k_cz$. Similarly, multiplying Eq. (4) by $\mathrm{e}^{\mathrm{i}k_cz}$ and integrating over the cross-sectional area of the sample, A, and the cavity length, $\mathscr{L}$, gives

$$\frac{\mathrm{d}\mathscr{E}_2}{\mathrm{d}t} = \frac{\mathrm{i}k_c\mu n}{2\epsilon_0}\left\langle S_2 + S_1\mathrm{e}^{\mathrm{i}\theta}\right\rangle. \quad (6)$$

So far we have considered the cavity as ideal i.e. without losses. In order to take account of finite losses at the mirrors and injected fields, we assume that the evolution of the complex field amplitudes $\mathscr{E}_{1,2}$ occurs on a timescale much longer than the cavity round-trip time $\mathscr{L}/c$. Therefore losses due to finite reflectivity mirrors ($R < 1$) can be represented by introducing a loss rate for each mode of $-T\mathscr{E}_{1,2}$ per round-trip, where $T = 1 - R$ is the mirror transmissivity i.e.

$$\left.\frac{\mathrm{d}\mathscr{E}_{1,2}}{\mathrm{d}t}\right|_{\text{losses}} = -\frac{T\mathscr{E}_{1,2}}{(\mathscr{L}/c)} = -\frac{cT}{\mathscr{L}}\mathscr{E}_{1,2}.$$

Similarly, the injected field can be represented as an increase in the cavity field at a rate $\sqrt{T}\mathscr{E}_{1,2}^{\text{IN}}$ per round-trip i.e.

$$\left.\frac{\mathrm{d}\mathscr{E}_{1,2}}{\mathrm{d}t}\right|_{\text{injected}} = \frac{\sqrt{T}\mathscr{E}_{1,2}^{\text{IN}}}{(\mathscr{L}/c)}\mathrm{e}^{-\mathrm{i}(\omega-\omega_c)t} = \frac{c\sqrt{T}}{\mathscr{L}}\mathscr{E}_{1,2}^{\text{IN}}\mathrm{e}^{-\mathrm{i}(\omega-\omega_c)t},$$

where $\omega_c = ck_c$ and we allow for the possibility that the oscillation frequency of the input field, ω, can be different from the cavity mode frequency ω_c. The equations describing the evolution of the complex field amplitudes therefore become

$$\frac{\mathrm{d}\mathscr{E}_1}{\mathrm{d}t} = \frac{\mathrm{i}ck_c\mu n}{2\epsilon_0}\left(\langle S_1\rangle + \left\langle S_2\mathrm{e}^{-\mathrm{i}\theta}\right\rangle\right) - \frac{cT}{\mathscr{L}}\left(\mathscr{E}_1 - \frac{\mathscr{E}_1^{\text{IN}}\mathrm{e}^{-\mathrm{i}(\omega-\omega_c)t}}{\sqrt{T}}\right), \quad (7)$$

$$\frac{\mathrm{d}\mathscr{E}_2}{\mathrm{d}t} = \frac{\mathrm{i}ck_c\mu n}{2\epsilon_0}\left(\langle S_2\rangle + \left\langle S_1\mathrm{e}^{\mathrm{i}\theta}\right\rangle\right) - \frac{cT}{\mathscr{L}}\left(\mathscr{E}_2 - \frac{\mathscr{E}_2^{\text{IN}}\mathrm{e}^{-\mathrm{i}(\omega-\omega_c)t}}{\sqrt{T}}\right). \quad (8)$$

2.2. Internal atomic dynamics

We assume the atoms have two internal energy states. The lower and upper energy states are labelled $|1\rangle$ and $|2\rangle$ respectively. The Bloch equations for the density matrix elements $\rho_{jk}, j, k = 1, 2$ are

$$\frac{\partial\rho_{21}}{\partial t} = -(\gamma_\perp + \mathrm{i}\omega_0)\rho_{21} + \frac{\mathrm{i}E\mu}{\hbar}(\rho_{11} - \rho_{22}), \quad (9)$$

$$\frac{\partial(\rho_{11} - \rho_{22})}{\partial t} = -\gamma_\parallel(\rho_{11} - \rho_{22}) + \frac{2\mathrm{i}E\mu}{\hbar}\left(\rho_{21} - \rho_{21}^*\right), \quad (10)$$

where $\mathbf{E} = E\hat{\mathbf{e}}$ and $\rho_{12} = \rho_{21}^*$. The dipole moment of the jth atom is

$$\mathbf{d}_j = \mu\big(\rho_{12}(z=z_j) + \text{c.c.}\big)\hat{\mathbf{e}}.$$

In order to be consistent with Eq. (3), we require

$$\rho_{21} = S_1(t)\mathrm{e}^{\mathrm{i}k_c(z-ct)} + S_2(t)\mathrm{e}^{-\mathrm{i}k_c(z+ct)}, \tag{11}$$

so

$$\frac{\mathrm{d}\rho_{21}(z=z_j(t))}{\mathrm{d}t} = \left(\frac{\mathrm{d}S_{1_j}}{\mathrm{d}t} + \mathrm{i}(k_c v_{z_j} - \omega_c)S_{1_j}\right)\mathrm{e}^{\mathrm{i}k_c(z_j(t)-ct)} + \left(\frac{\mathrm{d}S_{2_j}}{\mathrm{d}t} - \mathrm{i}(k_c v_{z_j} + \omega_c)S_{2_j}\right)\mathrm{e}^{-\mathrm{i}k_c(z_j(t)+ct)},$$

therefore Eq. (9) can be written as

$$\begin{aligned}\frac{\mathrm{d}S_{1_j}}{\mathrm{d}t}\mathrm{e}^{\mathrm{i}k_c z_j(t)} + \frac{\mathrm{d}S_{2_j}}{\mathrm{d}t}\mathrm{e}^{-\mathrm{i}k_c z_j(t)} &= \big(-\gamma_\perp + \mathrm{i}(\omega_c - \omega_0 - k_c v_{z_j})\big)S_{1_j}\mathrm{e}^{\mathrm{i}k_c z_j(t)} \\ &\quad + \big(-\gamma_\perp + \mathrm{i}(\omega_c - \omega_0 + k_c v_{z_j})\big)S_{2_j}\mathrm{e}^{-\mathrm{i}k_c z_j(t)} \\ &\quad + \frac{2\mathrm{i}\mu}{\hbar}\big(\mathscr{E}_1\mathrm{e}^{\mathrm{i}k_c z_j(t)} + \mathscr{E}_2\mathrm{e}^{-\mathrm{i}k_c z_j(t)}\big)D_j,\end{aligned} \tag{12}$$

where we have substituted for E using Eq. (1) and defined

$$D = \frac{\rho_{11} - \rho_{22}}{2}$$

i.e. D is half the population difference between the lower (1) and upper (2) energy states. Eq. (12) is always satisfied if

$$\frac{\mathrm{d}S_{1_j}}{\mathrm{d}t} = \big(-\gamma_\perp + \mathrm{i}(\omega_c - \omega_0 - k_c v_{z_j})\big)S_{1_j} + \frac{2\mathrm{i}\mu}{\hbar}\mathscr{E}_1 D_j, \tag{13}$$

$$\frac{\mathrm{d}S_{2_j}}{\mathrm{d}t} = \big(-\gamma_\perp + \mathrm{i}(\omega_c - \omega_0 + k_c v_{z_j})\big)S_{2_j} + \frac{2\mathrm{i}\mu}{\hbar}\mathscr{E}_2 D_j. \tag{14}$$

Substituting for E, ρ_{21} in Eq. (10) gives

$$\frac{\mathrm{d}D_j}{\mathrm{d}t} = -\gamma_\parallel\big(D_j - D^{\mathrm{eq}}\big) + \frac{\mathrm{i}\mu}{\hbar}\big[S_{1_j}\big(\mathscr{E}_1^* + \mathscr{E}_2^*\mathrm{e}^{\mathrm{i}\theta_j(t)}\big) + S_{2_j}\big(\mathscr{E}_1^*\mathrm{e}^{-\mathrm{i}\theta_j(t)} + \mathscr{E}_1^*\big) + \text{c.c.}\big], \tag{15}$$

where $D^{\mathrm{eq}} = 0.5$ in the absence of any external excitation of the atom, $\theta_j(t) = 2k_c z_j(t)$ and we have neglected terms varying as $\mathrm{e}^{\pm 2\mathrm{i}\omega_c t}$. Eqs. (13)–(15) describe the internal degrees of freedom of each atom under the influence of the two counter-propagating cavity modes. It can be seen that as well as containing the field amplitudes $\mathscr{E}_{1,2}$, the evolution of S_1, S_2 and D for each atom is also dependent on the position z and velocity v_z of the atom. Therefore in order to obtain a closed description of the atom + field system, we must also derive equations which describe the evolution of the atomic centre-of-mass motion for each atom.

2.3. Atomic centre-of-mass dynamics

We describe the position and momentum of each atom in the ensemble classically. Strictly speaking, this classical description is valid only when the temperature of the atoms is greater than the recoil temperature $T_{\mathrm{R}} = \hbar\omega_{\mathrm{r}}/k_{\mathrm{B}}$, where $\omega_{\mathrm{r}} = 2\hbar k_c^2/M$ is the recoil frequency, M is the atomic mass and k_{B} is the Boltzmann's constant. The axial force on the jth atom is given by

$$F_{z_j} = \mathbf{d}_j \cdot \left.\frac{\partial \mathbf{E}}{\partial z}\right|_{z=z_j} \tag{16}$$

which using Eqs. (1) and (3) becomes

$$F_{z_j} = \mathrm{i}k_c\mu\Big(\mathscr{E}_1 S_{2_j}^*\mathrm{e}^{\mathrm{i}\theta_j} - \mathscr{E}_2 S_{1_j}^*\mathrm{e}^{-\mathrm{i}\theta_j} + \mathscr{E}_1 S_{1_j}^* - \mathscr{E}_2 S_{2_j}^* - \text{c.c.}\Big). \tag{17}$$

The centre-of-mass motion (position and velocity) of each atom is then described by the equations

$$\frac{\mathrm{d}\theta_j}{\mathrm{d}t} = 2k_c v_{z_j}, \tag{18}$$

$$\frac{\mathrm{d}v_{z_j}}{\mathrm{d}t} = \frac{F_{z_j}}{M} = \frac{\mathrm{i}k_c\mu}{M}\Big(\mathscr{E}_1 S_{2_j}^*\mathrm{e}^{\mathrm{i}\theta_j} - \mathscr{E}_2 S_{1_j}^*\mathrm{e}^{-\mathrm{i}\theta_j} + \mathscr{E}_1 S_{1_j}^* - \mathscr{E}_2 S_{2_j}^* - \text{c.c.}\Big). \tag{19}$$

Eqs. (7), (8), (13)–(15), (18) and (19) constitute a closed set of evolution equations which completely describe the self-consistent interaction of an ensemble of two-level atoms with two counterpropagating cavity modes.

2.4. Universal scaling

We now introduce the scaled time, momentum and field amplitude variables

$$\bar{t} = \omega_{\mathrm{r}}\rho t, \qquad \bar{p} = \frac{Mv_z}{\hbar k_c \rho},$$

$$A_{1,2} = -\mathrm{i}\sqrt{\frac{2\epsilon_0}{n\hbar\omega\rho}}\mathscr{E}_{1,2},$$

the scaled transverse and longitudinal damping parameters

$$\Gamma_\perp = \frac{\gamma_\perp}{\omega_r\rho}, \qquad \Gamma_\parallel = \frac{\gamma_\parallel}{\omega_r\rho},$$

the scaled cavity-atom detuning and field-cavity detuning parameters

$$\Delta_c = \frac{\omega_c - \omega_0}{\omega_r\rho}, \qquad \delta_c = \frac{\omega - \omega_c}{\omega_r\rho},$$

and the scaled cavity line width

$$\kappa = \frac{cT}{\mathscr{L}\omega_r\rho}.$$

The parameter ρ is defined as

$$\rho = \left(\frac{\omega_c\mu^2 n}{2\epsilon_0\omega_r^2\hbar}\right)^{1/3} \tag{20}$$

and from the definition of $A_{1,2}$ can be regarded as a measure of the number of photons per atom in the cavity.

Rewriting the evolution equations (7), (8), (13)–(15), (18) and (19) in terms of these scaled variables we obtain

$$\frac{\mathrm{d}S_{1_j}}{\mathrm{d}\bar{t}} = \left[-\Gamma_\perp + \mathrm{i}\left(\Delta_c - \frac{p_j}{2}\right)\right]S_{1_j} - 2\rho A_1 D_j, \tag{21}$$

$$\frac{\mathrm{d}S_{2_j}}{\mathrm{d}\bar{t}} = \left[-\Gamma_\perp + \mathrm{i}\left(\Delta_c + \frac{p_j}{2}\right)\right]S_{2_j} - 2\rho A_2 D_j, \tag{22}$$

$$\frac{\mathrm{d}D_j}{\mathrm{d}\bar{t}} = -\Gamma_\parallel\left(D_j - D^{\mathrm{eq}}\right) + \rho\left[S_{1_j}\left(A_1^* + A_2^*\mathrm{e}^{\mathrm{i}\theta_j}\right) + S_{2_j}\left(A_1^*\mathrm{e}^{-\mathrm{i}\theta_j} + A_2^*\right) + \mathrm{c.c.}\right], \tag{23}$$

$$\frac{\mathrm{d}\theta_j}{\mathrm{d}\bar{t}} = p_j, \tag{24}$$

$$\frac{\mathrm{d}p_j}{\mathrm{d}\bar{t}} = -\left[S_{1_j}^*\left(A_1 - A_2\mathrm{e}^{-\mathrm{i}\theta_j}\right) + S_{2_j}^*\left(A_1\mathrm{e}^{\mathrm{i}\theta_j} - A_2\right) + \mathrm{c.c.}\right], \tag{25}$$

$$\frac{\mathrm{d}A_1}{\mathrm{d}\bar{t}} = \langle S_1\rangle + \left\langle S_2\mathrm{e}^{-\mathrm{i}\theta}\right\rangle - \kappa\left(A_1 - \frac{A_1^{\mathrm{IN}}}{\sqrt{T}}\mathrm{e}^{-\mathrm{i}\delta_c\bar{t}}\right), \tag{26}$$

$$\frac{\mathrm{d}A_2}{\mathrm{d}\bar{t}} = \langle S_2\rangle + \left\langle S_1\mathrm{e}^{\mathrm{i}\theta}\right\rangle - \kappa\left(A_2 - \frac{A_2^{\mathrm{IN}}}{\sqrt{T}}\mathrm{e}^{-\mathrm{i}\delta_c\bar{t}}\right). \tag{27}$$

Finally, defining the new field and polarisation variables:

$$\tilde{A}_{1,2} = A_{1,2}\mathrm{e}^{\mathrm{i}\delta_c t}, \qquad \widetilde{S}_{1,2} = S_{1,2}\mathrm{e}^{\mathrm{i}\delta_c t},$$

Eqs. (21)–(27) become

$$\frac{\mathrm{d}\widetilde{S}_{1_j}}{\mathrm{d}\bar{t}} = \left[-\Gamma_\perp + \mathrm{i}\left(\Delta - \frac{p_j}{2}\right)\right]\widetilde{S}_{1_j} - 2\rho\tilde{A}_1 D_j, \tag{28}$$

$$\frac{\mathrm{d}\widetilde{S}_{2_j}}{\mathrm{d}\bar{t}} = \left[-\Gamma_\perp + \mathrm{i}\left(\Delta + \frac{p_j}{2}\right)\right]\widetilde{S}_{2_j} - 2\rho\tilde{A}_2 D_j, \tag{29}$$

$$\frac{\mathrm{d}D_j}{\mathrm{d}\bar{t}} = -\Gamma_\parallel\left(D_j - D^{\mathrm{eq}}\right) + \rho\left[\widetilde{S}_{1_j}\left(\tilde{A}_1^* + \tilde{A}_2^*\mathrm{e}^{\mathrm{i}\theta_j}\right) + \widetilde{S}_{2_j}\left(\tilde{A}_1^*\mathrm{e}^{-\mathrm{i}\theta_j} + \tilde{A}_2^*\right) + \mathrm{c.c.}\right], \tag{30}$$

$$\frac{\mathrm{d}\theta_j}{\mathrm{d}\bar{t}} = p_j, \tag{31}$$

$$\frac{\mathrm{d}p_j}{\mathrm{d}\bar{t}} = -\left[\widetilde{S}_{1_j}^*\left(\tilde{A}_1 - \tilde{A}_2\mathrm{e}^{-\mathrm{i}\theta_j}\right) + \widetilde{S}_{2_j}^*\left(\tilde{A}_1\mathrm{e}^{\mathrm{i}\theta_j} - \tilde{A}_2\right) + \mathrm{c.c.}\right], \tag{32}$$

$$\frac{\mathrm{d}\tilde{A}_1}{\mathrm{d}\bar{t}} = \langle\widetilde{S}_1\rangle + \langle\widetilde{S}_2\mathrm{e}^{-\mathrm{i}\theta}\rangle - \kappa\left(\tilde{A}_1 - \frac{\tilde{A}_1^{\mathrm{IN}}}{\sqrt{T}}\right) + \mathrm{i}\delta_c\tilde{A}_1, \tag{33}$$

$$\frac{\mathrm{d}\tilde{A}_2}{\mathrm{d}\bar{t}} = \langle\widetilde{S}_2\rangle + \langle\widetilde{S}_1\mathrm{e}^{\mathrm{i}\theta}\rangle - \kappa\left(\tilde{A}_2 - \frac{\tilde{A}_2^{\mathrm{IN}}}{\sqrt{T}}\right) + \mathrm{i}\delta_c\tilde{A}_2, \tag{34}$$

where

$$\Delta = \Delta_c + \delta_c = \frac{\omega - \omega_0}{\omega_r\rho}$$

is the scaled field-atom detuning. Eqs. (28)–(34) are the working set of equations we will use to investigate dispersive OB in a cold atomic vapour. In what follows, we consider only a unidirectionally pumped cavity i.e. $\tilde{A}_1^{\mathrm{IN}} = 0$.

3. Dispersive optical bistability neglecting recoil

In this section, we show how the model derived reduces to the conventional model of dispersive OB [2] when the effects of atomic recoil are neglected ($\mathrm{d}\theta_j/\mathrm{d}\bar{t} = \mathrm{d}p_j/\mathrm{d}\bar{t} = 0$), and we consider only unidirectional radiation propagation in the cavity ($A_1 = 0$). In this limit, Eqs. (28)–(34) reduce to

$$\frac{\mathrm{d}\widetilde{S}_2}{\mathrm{d}\bar{t}} = (-\Gamma + \mathrm{i}\Delta)\widetilde{S}_2 - 2\rho\tilde{A}_2 D, \tag{35}$$

$$\frac{\mathrm{d}D}{\mathrm{d}\bar{t}} = -\Gamma\left(D - \frac{1}{2}\right) + \rho\left(\widetilde{S}_{2_j}\tilde{A}_2^* + \text{c.c.}\right), \tag{36}$$

$$\frac{\mathrm{d}\tilde{A}_2}{\mathrm{d}\bar{t}} = \widetilde{S}_2 - \kappa\left(\tilde{A}_2 - \tilde{A}_2^{\mathrm{eq}}\right) + \mathrm{i}\delta_c\tilde{A}_2, \tag{37}$$

where $\tilde{A}_2^{\mathrm{eq}} = \tilde{A}_2^{\mathrm{IN}}/\sqrt{T}$, we have assumed $\Gamma_\perp = \Gamma_\parallel = \Gamma$ and we have dropped the j subscript as $\widetilde{S}$ and D are independent of j.

The steady state solution of Eqs. (35)–(37) is

$$\widetilde{S}_2 = -\frac{2\rho\tilde{A}_2 D}{\Gamma - \mathrm{i}\Delta}, \tag{38}$$

$$D = \frac{1}{2} + \frac{\rho}{\Gamma}\left(\widetilde{S}_2\tilde{A}_2^* + \text{c.c.}\right), \tag{39}$$

$$\tilde{A}_2 = \frac{\kappa\tilde{A}_2^{\mathrm{eq}} + \widetilde{S}_2}{\kappa - \mathrm{i}\delta_c}. \tag{40}$$

Substituting for $\widetilde{S}_2$ in Eq. (40) using Eqs. (38) and (39) gives

$$\left(\kappa - \mathrm{i}\delta_c + \frac{\rho(\Gamma + \mathrm{i}\Delta)}{\Gamma^2 + \Delta^2 + 4\rho^2|\tilde{A}_2|^2}\right)\tilde{A}_2 = \kappa\tilde{A}_2^{\mathrm{eq}}. \tag{41}$$

In order to show the connection with previous work [2] we define the quantities

$$X = \left(\frac{2\rho|\tilde{A}_2|}{\Gamma}\right)^2, \qquad Y = \left(\frac{2\rho|\tilde{A}_2^{\mathrm{eq}}|}{\Gamma}\right)^2$$

and the parameters

$$C = \frac{\rho}{2\kappa\Gamma}, \quad \Delta' = \frac{\Delta}{\Gamma}, \quad \Theta = \frac{\delta_c}{\kappa}$$

which allows us to write Eq. (41) in the form

$$Y = X\left[\left(1 + \frac{2C}{1 + \Delta'^2 + X}\right)^2 + \left(\Theta - \frac{2C\Delta}{1 + \Delta'^2 + X}\right)^2\right]. \tag{42}$$

This expression relating the incident (Y) and transmitted (X) field intensities is identical to that given in Eq. (30) of Ref. [2]. In this paper we are concerned with dispersive bistability, so we take the dispersive limit $\Delta' \gg 1$. In this limit, and assuming that the atoms are only weakly excited ($X \ll \Delta'^2$), then Eq. (42) reduces to the so-called cubic model of dispersive OB [3]:

$$Y \approx X\left[1 + (B - AX)^2\right], \tag{43}$$

where

$$A = \frac{2C}{\Delta'^3} \quad \text{and} \quad B = \frac{2C}{\Delta'} - \Theta.$$

The conditions for the existence of dispersive OB are

(i) the function $Y(X)$ has an inflexion point ($\mathrm{d}^2Y/\mathrm{d}X^2 = 0$),
(ii) $\mathrm{d}Y/\mathrm{d}X < 0$ at the inflexion point.

Using Eq. (43) it can be shown that in order to satisfy these conditions we require $B > \sqrt{3}$ or

$$\left|\frac{\rho}{\Delta} - \delta_c\right| > \sqrt{3}\kappa$$

for dispersive bistability to occur.

An interesting feature with regard to what follows is the fact that the bistability curve $Y(X)$ as described by Eq. (43) is unaffected if both the field-atom detuning Δ and the field-cavity detuning δ_c change sign. The physical reason for this is that dispersive OB relies on the intensity dependence of the refractive index of the atomic medium. If $\delta_c \neq 0$, then in the absence of the atoms the cavity is weakly transmitting. To enable a highly transmitting state, the atomic detuning Δ must be chosen so that an increase in the intracavity intensity causes the refractive index of the medium to vary in such a way that the optical path length of the radiation in the sample tends towards the cavity length i.e towards resonance. The trans-

mitted intensity is therefore unaffected by a change in sign of both Δ and δ_c.

4. Dispersive optical bistability including recoil

4.1. Recoil-induced instability analysis

We now relax the restriction on the atomic motion imposed in the previous section and let the atoms move under the action of the EM fields in the cavity. If we attempt to find a steady state solution for the systems (29)–(32) and (34) when $\tilde{A}_1 = \widetilde{S}_1 = 0$, we find that

$$\widetilde{S}_{2_j} = -\frac{2\rho\tilde{A}_2 D_j}{\Gamma - \mathrm{i}(\Delta + p_j/2)},$$

$$D_j = D^{\mathrm{eq}} + \frac{\rho}{\Gamma}\left(\widetilde{S}_{2_j}\tilde{A}_2^* + \mathrm{c.c.}\right)$$

but

$$\frac{\mathrm{d}\theta_j}{\mathrm{d}\bar{t}} = p_j, \qquad \frac{\mathrm{d}p_j}{\mathrm{d}\bar{t}} = \widetilde{S}_{2_0}\tilde{A}_{2_0}^* + \mathrm{c.c.} \neq 0$$

so the velocity of each atom never reaches a true steady state. Physically, this is due to radiation pressure from the pump field ($\tilde{A}_2$). However, it can be seen from the above that if $p_j \ll \Gamma,\ \Delta\ \forall j$ the internal atomic variables (S_{2_j} and D_j) are in a quasi-steady state [14]. Therefore, for a short enough time, it should be possible to approximate the "initial" state of the system as a quasi-steady state where

$$\theta_j = \theta_{j_0} = (0, 2\pi],$$

$$p_j = 0,$$

$$\widetilde{S}_{2_j} = -\frac{\rho\tilde{A}_{2_0}(\Gamma + \mathrm{i}\Delta)}{\Gamma^2 + \Delta^2 + 4\rho^2|\tilde{A}_{2_0}|^2} \equiv \widetilde{S}_{2_0},$$

$$D_j = \frac{1}{2}\frac{\Gamma^2 + \Delta^2}{\Gamma^2 + \Delta^2 + 4\rho^2|\tilde{A}_{2_0}|^2} \equiv D_0,$$

$$\tilde{A}_1 = 0,$$

$$\tilde{A}_2 = \tilde{A}_{2_0}.$$

We now introduce small fluctuations about this quasi-steady state by defining

$$\theta_j(\bar{t}) = \theta_{j_0} + \delta\theta_j(\bar{t}), \tag{44}$$

$$p_j(\bar{t}) = \delta p_j(\bar{t}), \tag{45}$$

$$\widetilde{S}_{1_j}(\bar{t}) = \delta\widetilde{S}_{1_j}(\bar{t}), \tag{46}$$

$$\widetilde{S}_{2_j}(\bar{t}) = \widetilde{S}_{2_0} + \delta\widetilde{S}_{2_j}(\bar{t}), \tag{47}$$

$$D_j(\bar{t}) = D_0 + \delta D_j(\bar{t}), \tag{48}$$

$$\tilde{A}_1(\bar{t}) = \delta\tilde{A}_1(\bar{t}). \tag{49}$$

Note that we neglect fluctuations in the pump field, $\tilde{A}_2$, but not in $\widetilde{S}_2$. Substituting Eqs. (44)–(49) into the evolution Eqs. (28)–(33) and retaining only terms linear in the fluctuation variables we obtain

$$\frac{\mathrm{d}\delta S_{1_j}}{\mathrm{d}\bar{t}} = (-\Gamma + \mathrm{i}\Delta)\delta\widetilde{S}_{1_j} - 2\rho\delta\tilde{A}_1 D_0, \tag{50}$$

$$\frac{\mathrm{d}\delta S_{2_j}}{\mathrm{d}\bar{t}} = (-\Gamma + \mathrm{i}\Delta)\delta\widetilde{S}_{2_j} + \mathrm{i}\frac{\delta p_j}{2}\widetilde{S}_{2_0} - 2\rho\tilde{A}_{2_0}\delta D_j, \tag{51}$$

$$\frac{\mathrm{d}\delta D_j}{\mathrm{d}\bar{t}} = -\Gamma\delta D_j + \rho\Big(\delta\widetilde{S}_{1_j}\tilde{A}_{2_0}^*\mathrm{e}^{\mathrm{i}\theta_{j_0}} + \widetilde{S}_{2_0}\delta\tilde{A}_1^*\mathrm{e}^{-\mathrm{i}\theta_{j_0}} + \delta\widetilde{S}_{2_j}\tilde{A}_{2_0}^* + \mathrm{c.c.}\Big), \tag{52}$$

$$\frac{\mathrm{d}\delta\theta_j}{\mathrm{d}\bar{t}} = \delta p_j, \tag{53}$$

$$\frac{\mathrm{d}\delta p_j}{\mathrm{d}\bar{t}} = -\Big(\widetilde{S}_{2_0}^*\delta\tilde{A}_1\mathrm{e}^{\mathrm{i}\theta_{j_0}} - \delta\widetilde{S}_{1_j}^*\tilde{A}_{2_0}\mathrm{e}^{-\mathrm{i}\theta_{j_0}} - \delta\widetilde{S}_{2_j}^*\tilde{A}_{2_0} + \mathrm{c.c.}\Big), \tag{54}$$

$$\frac{\mathrm{d}\delta\tilde{A}_1}{\mathrm{d}\bar{t}} = \langle\delta\widetilde{S}_1\rangle - \mathrm{i}\widetilde{S}_{2_0}\langle\delta\theta\mathrm{e}^{-\mathrm{i}\theta_0}\rangle + \langle\delta\widetilde{S}_2\mathrm{e}^{-\mathrm{i}\theta_0}\rangle - (\kappa - \mathrm{i}\delta_c)\delta\tilde{A}_1, \tag{55}$$

where we have assumed $\langle\mathrm{e}^{-\mathrm{i}\theta_0}\rangle = 0$ as the atoms are initially uniformly distributed. It is possible to write Eqs. (50)–(55) in terms of a set of collective variables [14]:

$$b = -\mathrm{i}\langle\delta\theta\mathrm{e}^{-\mathrm{i}\theta_0}\rangle,$$

$$P = \langle\delta p\mathrm{e}^{-\mathrm{i}\theta_0}\rangle,$$

$$X = \langle\delta\widetilde{S}_1\rangle,$$

$$Y_1 = \langle\delta\widetilde{S}_2\mathrm{e}^{-\mathrm{i}\theta_0}\rangle,$$

$$Y_2 = \langle\delta\widetilde{S}_2^*\mathrm{e}^{-\mathrm{i}\theta_0}\rangle,$$

$$Z = \langle\delta D\mathrm{e}^{-\mathrm{i}\theta_0}\rangle.$$

This greatly reduces the number of linear equations to be solved from $5N+1$ to 7, irrespective of the number of atoms. These seven linear equations are obtained by differentiating each collective variable and using Eqs. (50)–(55), which results in

$$\frac{\mathrm{d}X}{\mathrm{d}\bar{t}} = -(\Gamma - \mathrm{i}\Delta)X - 2\rho\delta\tilde{A}_1 D_0, \tag{56}$$

$$\frac{\mathrm{d}Y_1}{\mathrm{d}\bar{t}} = \mathrm{i}\frac{S_{2_0}}{2}P - (\Gamma - \mathrm{i}\Delta)Y_1 - 2\rho\tilde{A}_{2_0}Z, \tag{57}$$

$$\frac{\mathrm{d}Y_2}{\mathrm{d}\bar{t}} = -\mathrm{i}\frac{S^*_{2_0}}{2}P - (\Gamma + \mathrm{i}\Delta)Y_2 - 2\rho\tilde{A}^*_{2_0}Z, \tag{58}$$

$$\frac{\mathrm{d}Z}{\mathrm{d}\bar{t}} = -\Gamma Z + \rho\left[\tilde{A}^*_{2_0}(X+Y_1) + \tilde{A}_{2_0}Y_2 + \delta\tilde{A}_1\widetilde{S}^*_{2_0}\right], \tag{59}$$

$$\frac{\mathrm{d}b}{\mathrm{d}\bar{t}} = -\mathrm{i}P, \tag{60}$$

$$\frac{\mathrm{d}P}{\mathrm{d}\bar{t}} = \tilde{A}^*_{2_0}(X+Y_1) + \tilde{A}_{2_0}Y_2 - \delta\tilde{A}_1\widetilde{S}^*_{2_0}, \tag{61}$$

$$\frac{\mathrm{d}\delta\tilde{A}_1}{\mathrm{d}\bar{t}} = X + \widetilde{S}_{2_0}b + Y_1 - (\kappa - \mathrm{i}\delta_c)\delta\tilde{A}_1. \tag{62}$$

At this point, we now assume that the atomic decay rate Γ is much greater than either the cavity decay rate κ or the magnitude of the field-cavity detuning δ_c i.e. $\Gamma \gg \kappa, |\delta_c|$. This approximation allows us to adiabatically eliminate the atomic variables X, Y_1, Y_2 and Z for times $\bar{t} \gg \Gamma^{-1}$, so that

$$X \approx -\frac{2\rho D_0}{\Gamma - \mathrm{i}\Delta}\delta\tilde{A}_1,$$

$$Y_1 \approx \frac{(\mathrm{i}/2)\widetilde{S}_{2_0}P - 2\rho\tilde{A}_{2_0}Z}{\Gamma - \mathrm{i}\Delta},$$

$$Y_2 \approx \frac{-(\mathrm{i}/2)\widetilde{S}^*_{2_0}P - 2\rho\tilde{A}^*_{2_0}Z}{\Gamma + \mathrm{i}\Delta},$$

$$Z \approx \frac{\rho\tilde{A}^*_{2_0}(X+Y_1) + \rho\tilde{A}_{2_0}Y_2 + \rho\widetilde{S}^*_{2_0}\delta\tilde{A}_1}{\Gamma}.$$

Solving for X, Y_1, Y_2 and Z and substituting in Eqs. (60)–(62), we obtain

$$\frac{\mathrm{d}b}{\mathrm{d}\bar{t}} = -\mathrm{i}P, \tag{63}$$

$$\frac{\mathrm{d}P}{\mathrm{d}\bar{t}} = \frac{2\rho\Gamma|\tilde{A}_{2_0}|^2}{\Delta^3}\left(P + \frac{4\rho^2\tilde{A}^*_{2_0}\delta\tilde{A}_1}{\Delta}\right) - 2\mathrm{i}\frac{\rho\tilde{A}^*_{2_0}\delta\tilde{A}_1}{\Delta}, \tag{64}$$

$$\frac{\mathrm{d}\delta\tilde{A}_1}{\mathrm{d}\bar{t}} = -\frac{\rho}{\Gamma - \mathrm{i}\Delta}\left[\delta\tilde{A}_1 + \mathrm{i}\frac{\tilde{A}_{2_0}}{2\Delta^2}(\Gamma + \mathrm{i}\Delta)P + \tilde{A}_{2_0}b\right] - (\kappa - \mathrm{i}\delta_c)\delta\tilde{A}_1, \tag{65}$$

where it has been assumed that Γ^2, $4\rho^2|\tilde{A}^2_{2_0}| \ll \Delta^2$. If we now look for solutions of Eqs. (63)–(65) with the form b, P, $\delta\tilde{A}_1 \propto \mathrm{e}^{\lambda\bar{t}}$ then it can be shown that λ satisfies

$$\lambda^3 + \mathrm{i}\frac{\rho}{\Delta}\lambda^2 - \frac{\rho^2|\tilde{A}_{2_0}|^2}{\Delta^3}\lambda - 2\mathrm{i}\frac{\rho^2|\tilde{A}_{2_0}|^2}{\Delta^2} = 0, \tag{66}$$

where for simplicity the limits $\Gamma/\Delta \to 0$, $\kappa/\Delta \to 0$ and $\delta_c/\Delta \to 0$ have been assumed. If we further assume that $|\lambda| \ll \rho/|\Delta|$ and $|\lambda| \ll |\Delta|$ then Eq. (66) reduces to the simple expression

$$\lambda^2 = \frac{2\rho|\tilde{A}_{2_0}|^2}{\Delta}. \tag{67}$$

It is clear from Eq. (67) that when $\Delta > 0$, the system is unstable, and both the probe field amplitude, $\delta\tilde{A}_1$ and the atomic density modulation or bunching, b, grow exponentially at a rate

$$g = \mathrm{Re}(\lambda) = \sqrt{\frac{2\rho}{\Delta}}|\tilde{A}_{2_0}|. \tag{68}$$

In contrast, when $\Delta < 0$, Eq. (67) shows that the system is stable and no amplification of the probe amplitude or bunching occurs.

It should be noted that the above result highlights a significant difference between the nature of dispersive OB in a cold system when the effects of atomic recoil are neglected and when they are included. In the previous section, it was shown that the bistable behaviour of the atom-field system was unchanged when the signs of both δ_c and Δ were changed. From Eq. (67), it can be seen that the behaviour of the system is now strongly dependent on the sign of Δ alone, regardless of the sign of δ_c.

4.2. Numerical results

In order to validate the results of the linear analysis of the previous section and to describe the nonlinear dynamics of the system, we require a numerical solution of Eqs. (28)–(34). The common parameters we use for our examples are $\rho = 200$, $\Gamma = 2.0$, $\kappa = 0.16$, $|\Delta| = 20$ and $|\delta_c| = 0.16$. A physical situation described by these parameters is that of a cold sample of rubidium vapour with length $L_s = 1$ mm and density $n_s = 9.0 \times 10^{10}$ cm^{-3}, enclosed in a ring cavity of length $\mathscr{L} \approx 1$ m consisting of mirrors with 99% reflectivity. The cavity is tuned close to resonance with the $5^2S_{1/2}$–$5^2P_{3/2}$ transition ($\lambda = 780$ nm).

4.2.1. No recoil

First of all, we consider the case where the effects of recoil are artificially 'switched-off' and the cavity supports unidirectional propagation only. In the numerical calculations this is done by setting $d\theta_j/d\bar{t} = dp_j/d\bar{t} = \tilde{A}_1 = \tilde{S}_1 = 0$ for all $\bar{t}$. We then integrate the remaining Eqs. (29), (30) and (34) for several values of the incident field amplitude $|\tilde{A}_2^{eq}|$ when $\Delta = -20$ and $\delta_c = -0.16$. Plotting a graph of $|\tilde{A}_2|^2$ when the system is at steady state against $|\tilde{A}_2^{eq}|^2$ for these parameters, we obtain the familiar bistability curve shown in Fig. 2. A similar bistability curve can also be obtained from a direct analytical solution of Eqs. (42) or (43). An interesting property of these equations is that their solutions are dependent only on the sign of the product $\Delta\delta_c$, and not the signs of Δ and δ_c individually. We confirm this numerically by repeating the above procedure using $\Delta = 20$ and $\delta_c = 0.16$, so that $\Delta\delta_c > 0$ as before. The resulting bistability curve is shown in Fig. 3 and is clearly identical to that in Fig. 2. In practice, such a change in Δ and δ_c would be effected by very small changes in the pump laser frequency and the length of the cavity. These changes are sufficiently small that the other parameters such as the sample density and therefore ρ are effectively constant.

4.2.2. The effect of atomic recoil

Let us now relax the restrictions imposed in the previous section and allow for the effects of atomic recoil and bidirectional propagation in the cavity. We choose a value of $|\tilde{A}_2^{eq}|$ such that we are operating in the bistable regime ($|\tilde{A}_2^{eq}| = 1$) and no input probe field ($\tilde{A}_1^{eq} = 0$). For the rubidium vapour example described before, this value of scaled

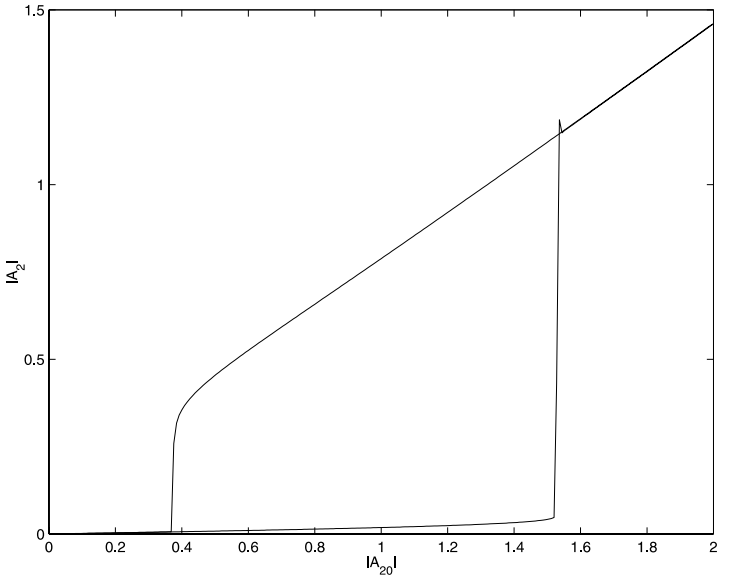

Fig. 2. Variation of $|\tilde{A}_2|$ with $|\tilde{A}_2^{eq}|$ when $\Delta = -20$, $\delta_c = -0.16$ and recoil is neglected.

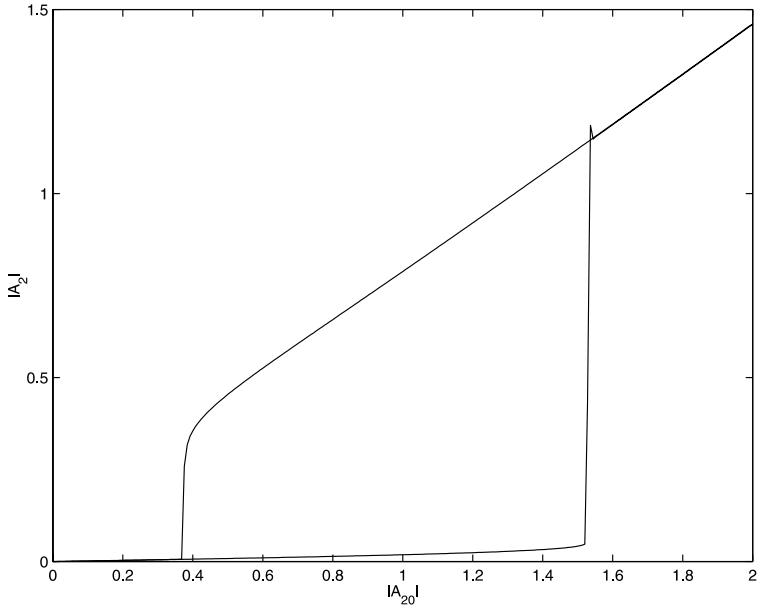

Fig. 3. Variation of $|\tilde{A}_2|$ with $|\tilde{A}_2^{\mathrm{eq}}|$ when $\Delta = 20$, $\delta_c = 0.16$ and recoil is neglected.

pump amplitude corresponds to an actual pump intensity of $I_2 = 1.4\ \mathrm{W\,cm^{-2}}$. We now investigate the temporal evolution of the EM fields and the atomic dynamics. The initial conditions are

$$\theta_j \in [0, 2\pi), \qquad p_j = \widetilde{S}_{1_j} = \widetilde{S}_{2_j} = 0 \quad \forall\, j,$$
$$D_j = 0.5 \quad \forall\, j, \qquad \tilde{A}_1 = \tilde{A}_2 = 10^{-4}$$

which corresponds to a cavity containing a collection of uniformly distributed, cold atoms in their ground state and very weak (noise) radiation fields.

The first case we investigate is that where $\Delta = -20$ and $\delta_c = -0.16$. Fig. 4 shows the evolution of the field intensities $|A_1|^2$ (solid line) and $|A_2|^2$ (dashed line) and of the modulus of the bunching parameter $b = \langle \mathrm{e}^{-\mathrm{i}\theta} \rangle$. The magnitude of b is a measure of the atomic density modulation on the atomic wavelength scale. It is clear that a uniform distribution in θ results in $|b| = 0$, whereas if all atoms are bunched at the same value of θ, then $|b| = 1$. It can be seen from Fig. 4 that the behaviour of the fields is very close to what would be expected if atomic recoil were neglected. After a short transient $\sim\Gamma^{-1}$, the pump field intensity $|\tilde{A}_2|^2$ attains a steady value which corresponds to the lower branch of the bistability curve in Fig. 2 when $|\tilde{A}_2^{\mathrm{eq}}| = 1$. The probe field intensity $|\tilde{A}_1|^2$ and the bunching parameter $|b|$ remain very small, indicating that the atoms remain essentially uniformly distributed in space.

Similar to the previous section, we now investigate the effect of changing the sign of both Δ and δ_c. Fig. 5 shows the evolution of the field intensities and the atomic density modulation when $\Delta = 20$ and $\delta_c = 0.16$. In contrast to the previous case, it can be seen that although for short times ($\bar{t} < 60$, $t < 3$ μs in the Rb example) the evolution is similar to what would be expected if atomic recoil were neglected, for longer times it is very different. Both the probe field intensity $|\tilde{A}_1|^2$ and the atomic density modulation $|b|$ are observed to grow exponentially until $|b| \sim 1$ and the probe intensity is comparable to that of the pump. This large value of $|b|$ implies a strongly modulated atomic density with a period $\lambda/2$ i.e. a large amplitude atomic density grating. At this point the pump amplitude $|\tilde{A}_2|$ undergoes a sudden transition to a higher steady state value. This steady state for $|\tilde{A}_2|$ is approximately equal to the higher branch of the bistability curve in Figs. 2 and 3. The lower branch of the bistability curve is therefore

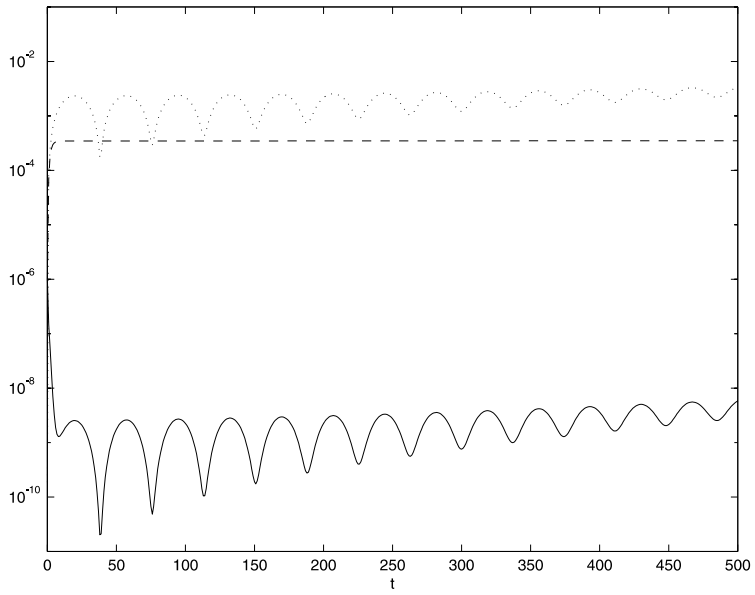

Fig. 4. Evolution of $|\tilde{A}_1|^2$ (—), $|\tilde{A}_2|^2$ (- - -) and $|b|$ ($\cdots$) as a function of $\bar{t}$ when $\Delta = -20$, $\delta_c = -0.16$ and recoil is included.

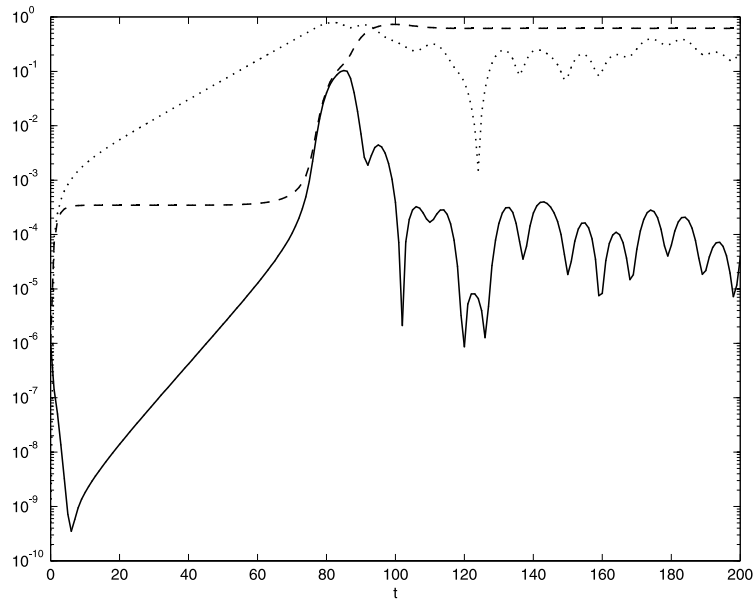

Fig. 5. Evolution of $|\tilde{A}_1|^2$ (—), $|\tilde{A}_2|^2$ (- - -) and $|b|$ ($\cdots$) as a function of $\bar{t}$ when $\Delta = 20$, $\delta_c = 0.16$ and recoil is included.

no longer truly stable when $\Delta > 0$, due to the growth of the atomic density modulation and the probe field.

The above strongly different behaviour of the system with a simultaneous change in sign of Δ and δ_c is consistent with the results of the linear analysis of Section 4.1, which predicted that the density modulation and probe amplitude will grow exponentially only if $\Delta > 0$. In addition, the growth rate of $|b|$ and $|\tilde{A}_1|$ as predicted by the

linear analysis (Eq. (68)) is 0.085 for the parameters used in this section. This is in good agreement with the corresponding growth rates as calculated from the full numerical integration (Fig. 5).

4.3. Physical mechanism

In this section, we attempt to give an intuitive physical explanation for the behaviour of the atoms and the radiation fields when the effects of atomic recoil are included. The main effects to be described are

- the strong dependence of the stability of the system on the sign of the atom-field detuning, Δ,
- the reason why unstable growth of the probe intensity and density grating causes the transition of the pump intensity from the low transmission branch to the high transmission branch of the bistability curve.

In order to obtain a simple explanation of these effects, let us examine the equations which describe the evolution of the scaled atomic momentum (32) and the probe field, $\tilde{A}_1$ (33). Let us assume that the atoms respond approximately linearly to the fields i.e. $2\rho\tilde{A}_2 \ll \Gamma$, Δ, and that their response is almost entirely dispersive i.e. $|\Delta| \gg \Gamma$, so that

$$D_j \approx \frac{1}{2} \quad \forall\, j,$$

$$S_{1_j,2_j} \approx -\mathrm{i}\frac{\rho\tilde{A}_{1,2}}{\Delta}$$

and the momentum and probe evolution equations (32) and (33) become

$$\frac{\mathrm{d}p_j}{\mathrm{d}\bar{t}} = -2\mathrm{i}\frac{\rho}{\Delta}\left(\tilde{A}_1\tilde{A}_2^*\mathrm{e}^{\mathrm{i}\theta_j} - \tilde{A}_1^*\tilde{A}_2\mathrm{e}^{-\mathrm{i}\theta_j}\right), \tag{69}$$

$$\frac{\mathrm{d}\tilde{A}_1}{\mathrm{d}\bar{t}} = -\mathrm{i}\frac{\rho\tilde{A}_1}{\Delta} - \mathrm{i}\frac{\rho\tilde{A}_2}{\Delta}\left\langle\mathrm{e}^{-\mathrm{i}\theta}\right\rangle - \kappa\tilde{A}_1 + \mathrm{i}\delta_c\tilde{A}_1. \tag{70}$$

The scaled force on each atom, as described by Eq. (69), can be described in terms of a position (θ_j) dependent potential

$$V_j = -\int \frac{\mathrm{d}p_j}{\mathrm{d}\bar{t}}\mathrm{d}\theta_j = \frac{2\rho}{\Delta}\left(\tilde{A}_1\tilde{A}_2^*\mathrm{e}^{\mathrm{i}\theta_j} + \tilde{A}_1^*\tilde{A}_2\mathrm{e}^{-\mathrm{i}\theta_j}\right). \tag{71}$$

The total scaled potential energy of the ensemble of atoms in the radiation fields is therefore

$$V = \sum_{j=1}^{N} V_j = N\langle V\rangle = \frac{2\rho N}{\Delta}\left(\tilde{A}_1\tilde{A}_2^*b^* + \tilde{A}_1^*\tilde{A}_2 b\right). \tag{72}$$

Assuming that $\mathrm{d}\tilde{A}_1/\mathrm{d}\bar{t} \ll \kappa\tilde{A}_1$, then Eq. (70) can be rearranged to give the probe field $\tilde{A}_1$ in terms of the pump field and the bunching parameter, b:

$$\tilde{A}_1 = -\frac{\rho\tilde{A}_2 b}{\rho - \mathrm{i}(\kappa - \mathrm{i}\delta_c)\Delta}. \tag{73}$$

Taking the limit of large dispersive susceptibility, $\rho/\Delta \gg \delta_c$, κ, Eq. (73) reduces to the particularly simple form

$$\tilde{A}_1 \approx -\tilde{A}_2 b. \tag{74}$$

Note that this expression suggests that if $|b| \approx 1$, a significant fraction of the pump intensity may be backscattered into the probe field from the atomic density grating. Substituting for $\tilde{A}_1$ in the expression for the potential energy of the system (72) gives

$$V = -\frac{4N\rho|\tilde{A}_2|^2|b|^2}{\Delta}. \tag{75}$$

This expression now allows us to see how the behaviour of the system is altered when the sign of the pump-atom detuning, Δ, is changed: When $\Delta > 0$, then the potential energy of the system decreases as $|b|$ is increased and is a minimum when $|b| = 1$, corresponding to a perfectly bunched atomic sample. Therefore when $\Delta > 0$ it is energetically favourable for the atoms to bunch strongly and consequently (from Eq. (74)) amplify the probe field. In contrast, when $\Delta < 0$ the potential energy of the system increases as $|b|$ is increased. The potential energy is minimised when $|b| = 0$, so it is energetically favourable for the atoms to remain uniformly spatially distributed and the probe field consequently does not grow.

A simple physical picture illustrating the reason for this behaviour can be obtained by considering a density modulation or bunching around a phase ϕ in the ponderomotive potential so that the bunching parameter $b = |b| \exp(-i\phi)$, where $|b|$ is arbitrary and $0 < \phi \leqslant 2\pi$. The potential energy of the jth atom is given by

$$V_j = -\frac{4\rho|\tilde{A}_2|^2}{\Delta}|b|\cos(\theta_j - \phi),$$

where Eqs. (71) and (74) have been used. It can be seen that when $\Delta > 0$, this potential has a minimum at $\theta_j = \phi$. Consequently as the jth atom moves towards the potential minimum, it reinforces the initial density modulation, leading to unstable growth of the atomic bunching and the probe field. In contrast, when $\Delta < 0$, the potential V_j has a minimum at $\theta_j = \phi + \pi$. As the jth atom moves towards the potential minimum, it moves towards a position π out of phase with the position which the atoms are currently bunched around. Therefore the atomic bunching is reduced from its initial value. The atomic bunching and the probe field can never grow strongly when $\Delta < 0$ because the probe field phase and consequently the ponderomotive potential continuously shift so as to counteract any density modulation which develops in the atomic medium.

Let us now consider how the existence of an atomic density grating affects the evolution of the pump field. In order to do this, we again assume that the atoms respond linearly to the fields and that $|\Delta| \gg \Gamma$. Consequently, the pump evolution Eq. (34) can be reduced to

$$\frac{d\tilde{A}_2}{d\bar{t}} = -i\frac{\rho\tilde{A}_2}{\Delta} - i\frac{\rho\tilde{A}_1}{\Delta}\langle e^{i\theta}\rangle - \kappa\left(\tilde{A}_2 - \tilde{A}_2^{eq}\right) + i\delta_c\tilde{A}_2.$$

If we now assume that that, as for the probe, the pump evolution is very slow i.e. $d\tilde{A}_2/d\bar{t} \ll \kappa\tilde{A}_2$, then this expression can be reduced to a relation between the intracavity pump field $\tilde{A}_2$ and the input pump field $\tilde{A}_2^{eq}$:

$$\left[\kappa - i\delta_c + i\frac{\rho}{\Delta}(1 - |b|^2)\right]\tilde{A}_2 \approx \kappa\tilde{A}_2^{eq}.$$

Using the variables X, Y and the parameters C, Δ' and Θ defined in Section 3, the above expression can be written as

$$Y = X\left[1 + \left(\Theta - \frac{2C}{\Delta'}(1 - |b|^2)\right)^2\right]. \tag{76}$$

It can be seen that the effect of increasing the bunching parameter, b, is to reduce the effective dispersive susceptibility of the atomic medium i.e. the term proportional to C in Eq. (76). In this sense the effect of increased atomic bunching is similar to that of an increase in intracavity pump intensity, X, in the absence of recoil (compare Eq. (76) with the corresponding relation (42) when $\Delta' \gg 1$). As the effective dispersive susceptibility of the atomic sample is reduced by bunching, bunched atoms appear more highly transmitting to the input pump field than an unbunched atomic sample. The recoil-induced instability, which occurs when $\Delta > 0$, causes exponential growth of the atomic bunching until eventually the atoms are sufficiently bunched ($|b| \sim 1$) that the pump transmission jumps from the low $\rightarrow$ high transmission state.

4.4. Doppler broadening

Up to this point, we have assumed that the atomic sample under consideration is 'cold', with effectively zero temperature initially. In this section we consider the effects of a finite thermal momentum spread on the recoil-induced instability described in the previous sections using a numerical analysis.

We assume a Gaussian momentum distribution such that the probability of finding an atom with a value of scaled initial momentum, p_0, in the range $p_0 \rightarrow p_0 + dp_0$ is $f(p_0)dp_0$, where

$$f(p_0) = \frac{1}{\sqrt{2\pi}\sigma}\exp\left(-\frac{p_0^2}{2\sigma^2}\right)$$

and

$$\sigma = \frac{Mv_{rms}}{\hbar k_c \rho} = \frac{\sqrt{3Mk_B T}}{\hbar k_c \rho}, \tag{77}$$

where T is the temperature of the atomic sample and we have used the fact that $(1/2)Mv_{rms}^2 = (3/2)k_B T$.

Fig. 6 shows a graph of the maximum value of $\tilde{A}_2$ as calculated from a numerical solution of Eqs. (28)–(34) when $\Delta = 20$ and $\delta_c = 0.16$ for several values of σ. All other parameters are the same as in

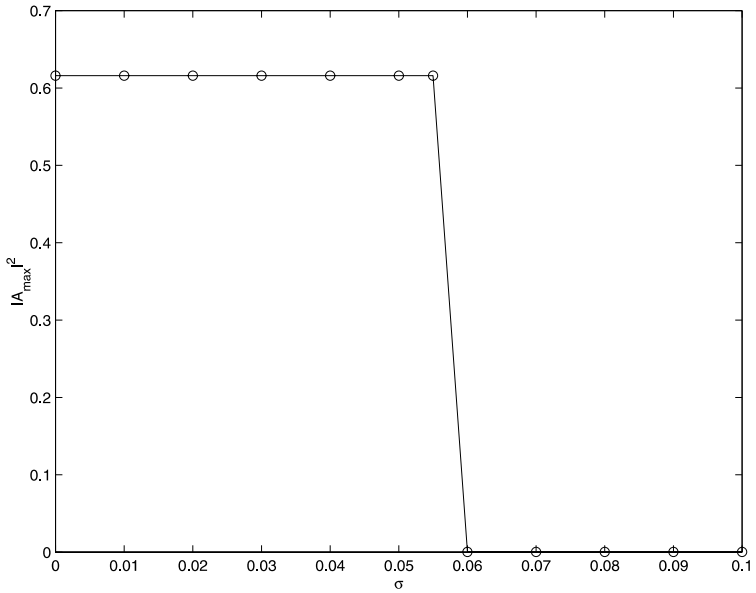

Fig. 6. Variation of $|\tilde{A}_2|^2$ with σ when $\Delta = 20$, $\delta_c = 0.16$ and recoil is included.

the previous section. It can be seen that when $\sigma > 0.06$ approximately, the pump intensity is unable to 'jump' to the high transmission state. This can be explained in simple terms by considering a collection of atoms perfectly bunched, so that $|b| = 1$ initially. In the absence of any radiation fields, the atoms evolve freely maintaining their initial momenta, so $p(\bar{t}) = p_0$ and $\theta(\bar{t}) = p_0\bar{t}$. The evolution of the bunching parameter as a function of $\bar{t}$ can then be evaluated analytically as

$$|b(\bar{t})| = \left| \int_{-\infty}^{\infty} f(p_0) \mathrm{e}^{-\mathrm{i}\theta} \mathrm{d}p_0 \right| = \exp\left(-\frac{\sigma^2 \bar{t}^2}{2} \right).$$

The effect of a thermal velocity spread i.e. temperature is therefore to cause a decay of the atomic density grating amplitude on a timescale σ^{-1}. As the recoil-induced instability results in amplification of the density grating amplitude on a timescale g^{-1}, it would be expected that the effect of temperature will quench the recoil-induced instability of the lower branch of the bistability curve when $\sigma \approx g$ or greater i.e. if $\sigma \approx \sqrt{2\rho/\Delta}|\tilde{A}_{2_0}|$, which for our example is 0.08. This agrees well with the results shown in Fig. 6, which shows that the recoil-induced instability is stabilised when $\sigma \geqslant 0.06$. This upper threshold for σ, the width of the velocity distribution, defines the temperature limit above which the recoil-induced effects described in the previous sections will be 'washed out' by thermal velocity spread. For our example involving a sample of cold Rb vapour, this maximum value for σ corresponds to a temperature of approximately 27μ K.

5. Conclusions

We have investigated OB of a dispersive system of two-level atoms enclosed in a bidirectional ring cavity. In contrast to previous analyses of dispersive OB we have included the atomic centre-of-mass motion, which is allowed to evolve in a self-consistent way under the action of the counterpropagating radiation fields within the cavity. It is well known that a collection of atoms enclosed in a ring cavity which is pumped unidirectionally can display bistable pump transmission due to the dispersive response of the atoms. When the effects of atomic recoil were neglected in our model this was indeed observed. In general the existence of this bistable regime is not strongly dependent on the sign of the atom-field detuning, Δ. When the effects of atomic recoil were included however, the

situation changed dramatically. We presented an example where for a red-detuned pump field ($\Delta < 0$), the situation is similar to the case without recoil, with unidirectional propagation in the cavity and two steady pump transmission states. However, for a blue-detuned pump ($\Delta > 0$) the system is unstable, leading to exponential growth of the counterpropagating radiation field and an atomic density modulation. This density modulation reduces the effective dispersive susceptibility of the atomic sample, causing the pump to "jump" from the low $\rightarrow$ high transmission state. It is expected that these effects should be observable in e.g. a cold ($T < 30\mu$ K), dense ($n \sim 10^{11}$ cm^{-3}) sample of Rb, enclosed in a high quality ring cavity ($R \approx 99\%$).

Acknowledgements

The authors would like to thank the Royal Society of Edinburgh and the EPSRC for support of GRMR and BWJM^{c}N respectively.

References

[1] R. Bonifacio, L. Lugiato, Opt. Commun. 19 (1976) 172.
[2] L. Lugiato, Prog. Opt. XXI (1984) 69 and references therein.
[3] H.M. Gibbs, S.L. McCall, T.N.C. Venkatesan, Phys. Rev. Lett. 36 (1976) 113.
[4] R. Bonifacio, B.W.J. McNeil, N. Piovella, G.R.M. Robb, Phys. Rev. A 61 (2000) 3807.
[5] R. Bonifacio, B.W.J. McNeil, N. Piovella, G.R.M. Robb, Opt. Commun. 179 (2000) 559.
[6] E. Abraham, S.D. Smith, Rep. Prog. Phys. 45 (1982) 815 and references therein.
[7] R. Bonifacio, L. De Salvo Souza, Nucl. Instr. Meth. Phys. Res. A 341 (1994) 360.
[8] R. Bonifacio, L. De Salvo, L.M. Narducci, E.J. D'Angelo, Phys. Rev. A 50 (1994) 1716.
[9] P.R. Berman, Phys. Rev. A 59 (1999) 585.
[10] M.G. Moore, P. Meystre, Phys. Rev. A 58 (1998) 3248.
[11] R. Bonifacio, B.W.J. McNeil, G.R.M. Robb, Opt. Commun. 161 (1999) 1.
[12] G.R.M. Robb, R. Bonifacio, B.W.J. McNeil, Phys. Rev. A 61 (2000) 1801.
[13] B.W.J. McNeil, G.R.M. Robb, R. Bonifacio, N. Piovella, Europhys. Lett. 49 (2000) 316.
[14] L. Desalvo, R. Cannerozzi, R. Bonifacio, E.J. D'Angelo, L.M. Narducci, Phys. Rev. A 52 (1995) 2342.